Additively manufactured shape-morphing implants for the treatment of acetabular defects

Moosabeiki, V.; Leeflang, M.A.; Gerbers, J.G.; Jong, P.H. de; Broekhuis, D.; Agarwal, Y.; ... ; Zadpoor, A.A.

Acta Biomaterialia 203 (2025) 358–368

Contents lists available at ScienceDirect

Acta Biomaterialia

journal homepage: www.elsevier.com/locate/actbio

Full length article

Additively manufactured shape-morphing implants for the treatment of acetabular defects

Vahid Moosabeiki [a,*], Marius A. Leeflang [a], Jasper G. Gerbers [b], Pier H. de Jong [a], Demien Broekhuis [b], Yash Agarwal [c], Jagathes N. Ganesen [c], Bart L. Kaptein [b], Rob G.H.H. Nelissen [b], Mohammad J. Mirzaali [a,*], Amir A. Zadpoor [a,b,*]

[a] Department of Biomechanical Engineering, Faculty of Mechanical Engineering, Delft University of Technology (TU Delft), Mekelweg 2, 2628 CD, Delft, The Netherlands
[b] Department of Orthopaedics, Leiden University Medical Center, Leiden, The Netherlands
[c] Synbone AG, Switzerland

ARTICLE INFO

Keywords:
Acetabular defect
3D printing
Flexible mesh
Kinematic structure
Shape matching
Patient-specific implant
Biomechanical testing

ABSTRACT

Acetabular defects pose significant challenges in orthopedic surgery, particularly in revision total hip arthroplasty (THA). Here, we design, additively manufacture, and evaluate shape-morphing porous implants with kinematic structures to address these defects. Three defect types were examined using synthetic hemipelvis models: posterior wall, cranial-posterior combination, and central-posterior defects. The implants were secured with screws and bone cement, and their surface conformity was assessed through micro computed tomography (μCT). Biomechanical performance was evaluated under quasi-static compression and cyclic loading conditions. Results demonstrated high surface conformity of the flexible mesh across all defect types, with minimal differences from healthy acetabula (< 10 mm). The mesh implants exhibited strong load-bearing capacity, with failures occurring only in the pubic region of the hemipelvis, while both the implants and mesh-cement interfaces remained intact. The implants withstood cyclic loading simulating half the body weight of a 80 kg patient for >1000,000 loading cycles with no evidence of fatigue failure, further confirming their durability. These findings suggest that the flexible mesh implant provides a potential solution for complex acetabular defects, offering anatomical conformity and mechanical stability, even in cases where conventional mesh grafts might be inadequate. Future studies, including cadaveric testing and clinical trials, are necessary to further validate these results in (pre-)clinical settings.

Statement of significance: This study addresses the need for adaptable solutions to complex acetabular defects in revision total hip arthroplasty (THA). Traditional implants struggle to conform to severe bone loss and irregular geometries, risking suboptimal fit, and implant migration. We introduce a 3D-printed, shape-morphing porous implant with kinematic structures, offering high anatomical conformity, mechanical robustness, and support for bone graft integration. Combining the adaptability of patient-specific implants with the efficiency of standard designs, this implant reduces lead times while enabling a tailored fit. This innovative approach provides a reliable solution for managing complex defects, addressing limitations of conventional implants, and improving outcomes in orthopedic reconstruction.

1. Introduction

Acetabular defects, involving structural damage or deformities in the acetabulum, pose significant challenges in orthopedic surgery. These defects can result from trauma, infection, tumor resection, or previous procedures like total hip arthroplasty (THA) [1,2]. Addressing bone deficiency during revision THA is particularly challenging for surgeons, but also managing severe acetabular deficiencies after infection or bone deformities after acetabular fractures [3]. The primary goals of acetabular reconstruction are to create a stable and durable fixation for a new acetabular component, restore the center of rotation, and, where possible, rebuild bone stock [4,5]. Effective management of these defects is essential to restore hip joint function and improve patient mobility [4,6–12]. However, traditional approaches, including standard

* Corresponding authors.
E-mail addresses: v.moosabeiki@tudelft.nl (V. Moosabeiki), m.j.mirzaali@tudelft.nl (M.J. Mirzaali), a.a.zadpoor@tudelft.nl (A.A. Zadpoor).

https://doi.org/10.1016/j.actbio.2025.07.018
Received 9 December 2024; Received in revised form 2 July 2025; Accepted 3 July 2025
Available online 5 July 2025

implants and grafting techniques, often fail to achieve precise anatomical fit and stable fixation, leading to less favorable outcomes and higher revision rates [13–15].

Standard revision hardware (cups, shells, crosses, trabecular metal augmentations, mesh-bone impaction combination) are generally designed to fit a wide range of patients but lack the necessary customization for unique anatomical variations. These generalized implants could result in poor implant positioning, hip instability, and potential increased wear, compromising surgical outcomes [16]. In response to these challenges, recent advancements in acetabular implant design, mainly through additive manufacturing (=3D printing) technology, have shown promise in managing complex acetabular defects [17–21]. Custom-made 3D printed acetabular components in THA have demonstrated encouraging results, especially in patients with severe bone defects [15,22–25]. Custom 3D printed triflange implants have also been evaluated for massive acetabular defects, both with and without pelvic discontinuity, resulting in high implant survivorship and significant functional improvements [5,20,25,26]. Custom 3D printed implants have demonstrated effective osseointegration and implant stability, particularly in complex revision surgeries, providing a reliable solution for challenging cases [5,25,27].

Despite the benefits, patient-specific implants present challenges. Although they offer superior anatomical conformity, they are often time-consuming and costly to produce [28,29]. The manufacturing process requires extensive preoperative planning, detailed imaging, and modeling, which can delay surgery and increase overall treatment costs [28,30]. Furthermore, the high cost of producing a unique implant for each patient may not be feasible in many healthcare settings, limiting their widespread adoption. Additionally, unlike bone impaction grafting (BIG) with mesh backing, patient-specific implants do not replenish bone stock, which is essential for long-term structural integrity and support [31].

Recent developments in shape-matching implants have sought to improve functional performance and production efficiency [28,32] to overcome these limitations. One such innovation involves shape-morphing implants, which adapt to complex anatomical geometries using advanced 3D and 4D printing techniques [33–37]. These implants conform to the patient's unique anatomy during surgery and lock into place, providing a customized fit without requiring extensive preoperative planning [38–40]. This approach blends the advantages of patient-specific and standard implants, offering a tailored fit and enhanced mechanical stability while reducing production time and costs. Shape-matching implants hold significant potential to advance orthopedic reconstruction by optimizing anatomical conformity and streamlining production processes. Additionally, these shape matching implants offer the possibility of expanding the use of bone impaction grafting (*i.e.,* host bone substitutes eventually the allograft bone) to address larger acetabular defects such as Paprosky IIIA and B [10,24,41].

We proposed the concept of "metallic clay", a design approach that enables medical devices, particularly orthopedic implants, to exhibit both shape-morphing and shape-locking capabilities [38]. Using this concept, this study aims to evaluate the design, manufacturing, and biomechanical performance of a 3D printed shape-morphing mesh implant with kinematic structures that combines the benefits of both standard and patient-specific implants. The kinematic mesh is designed as a generic implant capable of conforming to various patient anatomies, providing a patient-specific fit without the need for individualized manufacturing. This approach offers a versatile, cost-effective, and timely solution for managing acetabular defects.

The 3D printed flexible mesh implant was designed to adapt to the contours of the acetabulum and cover the acetabular defect. Furthermore, it could be effectively fixed to the intact acetabular bone using screws and bone cement. This design aimed to provide superior surface conformity and mechanical stability compared to conventional metal mesh implants [42]. To evaluate this approach, a series of experiments under physiologically relevant conditions were conducted using synthetic hemipelvis models with three distinct types of defects: (i) a large posterior acetabular wall defect, (ii) a combination of cranial and posterior acetabular wall defects, and (iii) central and posterior defects to replicate a Paprosky IIIB defect [42]. These models simulated the surgical procedure and implant placement. Post-operative evaluations included CT scanning to assess mesh conformity to the acetabular surface and mechanical testing to evaluate the implants' biomechanical performance under quasi-static and cyclic loading.

Compared to conventional acetabular metal mesh [42–44], and other flexible solutions like Noviomagus revision meshes [45], our flexible mesh design may significantly improve anatomical conformity when reconstructing large defects, as well as at sites where conventional metal mesh yields less favorable results [42]. This is likely due to the inferior mechanical stability of traditional options, which is addressed by our 3D printed shape-morphing implant, potentially improving overall surgical outcomes as well. Traditional metal meshes, which are flexible and manually shaped during surgery, are effective for smaller defects but often fall short in larger, more complex cases due to their inability to conform precisely to irregular geometries. Their flexibility can also lead to uneven load distribution and gaps between the mesh and bone [42]. Similarly, while Noviomagus meshes provide pre-shaped configurations that reduce intraoperative adjustments, their adaptability to highly irregular defect geometries is limited. In contrast, our flexible mesh is designed to conform more naturally to the defect and becomes rigid, potentially improving fit and stability. Once fixed, the mesh becomes rigid enough to withstand pressurized BIG, further enhancing its ability to accommodate larger volumes of graft material and promoting improved osseointegration and long-term mechanical stability (Supplementary Videos 1–4). This adaptability could enhance osseointegration and structural support in large or complex defects where conventional wire mesh may fall short.

This research addresses the critical need for innovative solutions in managing challenging acetabular defects by leveraging 3D printing technology. The primary hypothesis of this study is that a flexible, generic implant can effectively cover large acetabular defects that standard metal meshes cannot support while eliminating the need for costly and time-consuming patient-specific designs. By creating a flexible, generic implant capable of adapting to individual large anatomic defects, which is also stable and durable once in place, we aimed to overcome the limitations of standard flexible metal meshes and patient-specific implants. The outcomes of this study have the potential to enhance clinical practice by providing a customizable, effective, and economically viable option for patients with complex acetabular defects.

2. Materials and methods

2.1. Implant design and manufacturing

The shape-morphing implant was designed using computer-aided design (CAD) software, SolidWorks 2023 (Dassault Systèmes, France), to conform to various acetabular geometries (Figs. 1a and b). The design process involved creating a mesh structure with flexibility and strength suitable for anatomical adaptation and high enough load-bearing capacity. The hexagonal pattern (Fig. 1b) was chosen as the optimal design due to its uniform load distribution and structural efficiency, which are critical for orthopedic applications. To optimize the design, we developed in-house MATLAB code to simulate the kinematic behavior of the mesh and assess its ability to conform to curved surfaces. These simulations, combined with experimental testing, informed the selection of strut length, strut thickness, body size, and overall geometry, ensuring the mesh could adapt to complex anatomical geometries while providing sufficient mechanical support. The full details of the optimization process will be published separately as part of an ongoing study.

The mesh implants were 3D printed using plasma atomized Titanium alloy (Ti-6Al-4 V ELI) powder (AP&C Inc, Canada), with particle sizes

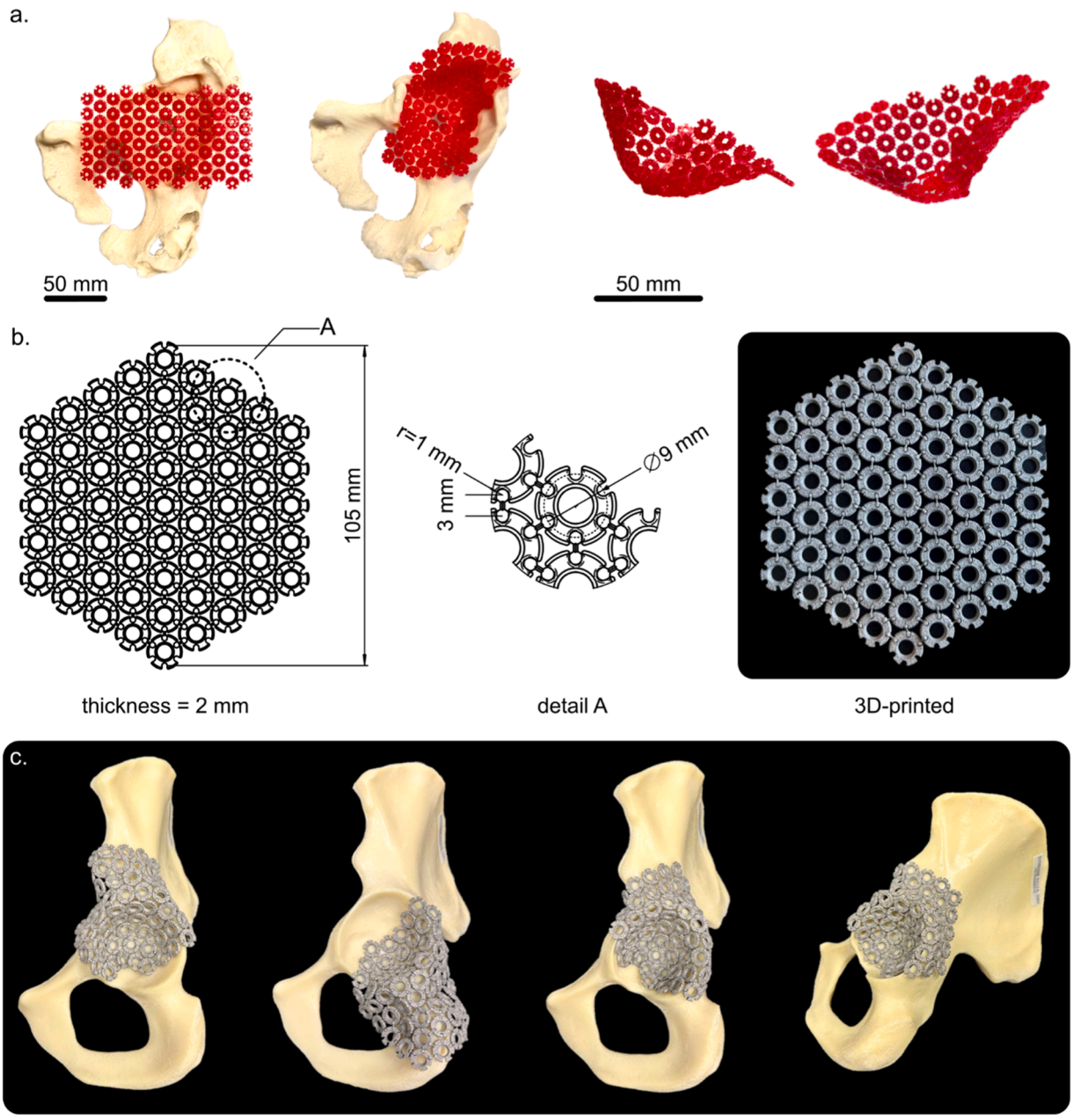

Fig. 1. Design and application of the flexible mesh implant for acetabular reconstruction. (a) Perspective view of the flexible mesh illustrating its adaptability and conformity to the acetabular defect. The mesh was fabricated using PolyJet printing technology. (b) A detailed schematic drawing of the mesh design. The right panel shows a 3D printed version of the mesh structure. (c) The flexible mesh implant integrated into different regions of the acetabulum of synthetic pelvis models, demonstrating surface conformity and coverage.

ranging from 10 to 45 μm. A high-resolution selective laser melting (SLM) 3D printer (ReaLizer SLM125, ReaLizer GmbH, Paderborn, Germany) was employed to manufacture the implants at the Additive Manufacturing Lab at Delft University of Technology. Considering the constraints of the additive manufacturing process, the implants were positioned lying flat on the print bed to ensure that the functional surfaces of the joint could be printed concomitantly without requiring support structures. This orientation allowed the entire implant to be printed in one go using the maximum build plate size of the SLM machine, making it fully functional after removing the build plate and completing ultrasonic cleaning. The design is inherently scalable, allowing the number of units and the overall size of the mesh to be adjusted based on the size of the defect and the specific anatomical requirements of the patient. In clinical practice, the mesh can be either printed in a few different sizes (to be trimmed to the required size during the surgery) or be customized by adding or removing units during the design phase. Additionally, the cross-sections of the rod end, connecting the spherical components, were designed in a rhombus shape to prevent warping.

2.2. Synthetic hemipelvis models

For this study, synthetic structurally calibrated hemipelvis models representing the left side of the pelvis, each with an acetabular diameter of 52 mm, were used to simulate realistic clinical scenarios and evaluate the performance of the 3D printed flexible mesh implants. Synthetic hemipelvis models (Synbone AG, Switzerland) were chosen for their consistency and ability to simulate specific defect geometries, which was critical for evaluating the shape-morphing capabilities of the implant. While these models do not fully replicate the mechanical properties of

human bone, they provide a controlled environment for initial testing.

Three different types of defects were represented to cover a range of clinical situations, from moderate to severe acetabular defects (Fig. 2). The first model simulated a posterior acetabular wall defect (Model 4122, Synbone AG, Switzerland). The second model featured a combination of cranial and posterior acetabular wall defects (Model 4123, Synbone AG, Switzerland), representing a more complex scenario involving extensive bone loss across multiple regions of the acetabulum. The third model was a modified healthy hemi-pelvis (Model 4032, Synbone AG, Switzerland) with central and posterior defects to replicate a Paprosky IIIB defect. Paprosky IIIB defects are characterized by substantial bone loss, compromising the structural integrity of the acetabulum and surrounding pelvic regions [10,24]. These defects pose significant challenges in reconstruction due to the extensive nature of bone loss and the difficulty in achieving stable fixation.

2.3. Surgical implementation

An experienced hip surgeon (JGG) performed the simulated surgeries. The surgical procedure for implanting the flexible mesh involved securing the mesh to the acetabulum of the synthetic hemipelvis models (Fig. 2 and Supplementary Videos 1–4). The acetabulum was prepared, and reamed using increasing size reamers to suitable depth (*i.e.,* final reamer size of 56 mm) . To improve cement integration and ensure a secure fit, ten to fifteen holes were drilled to a depth of 5-10 mm within the acetabular surface. The mesh was then carefully positioned over the defect area to ensure optimal coverage and fit. Once positioned correctly, the mesh was fixed in place using titanium cortical screws (AO large fragment screws, Depuy Synthes, Switzerland) with a diameter of 4.5 mm. The length of the screws varied between 24 mm and 40 mm, depending on the specific anatomical requirements of each defect model. The acetabulum was then carefully cleaned to remove any loose debris.

Bone cement (Polymethyl methacrylate, PMMA, Optimpac® 60

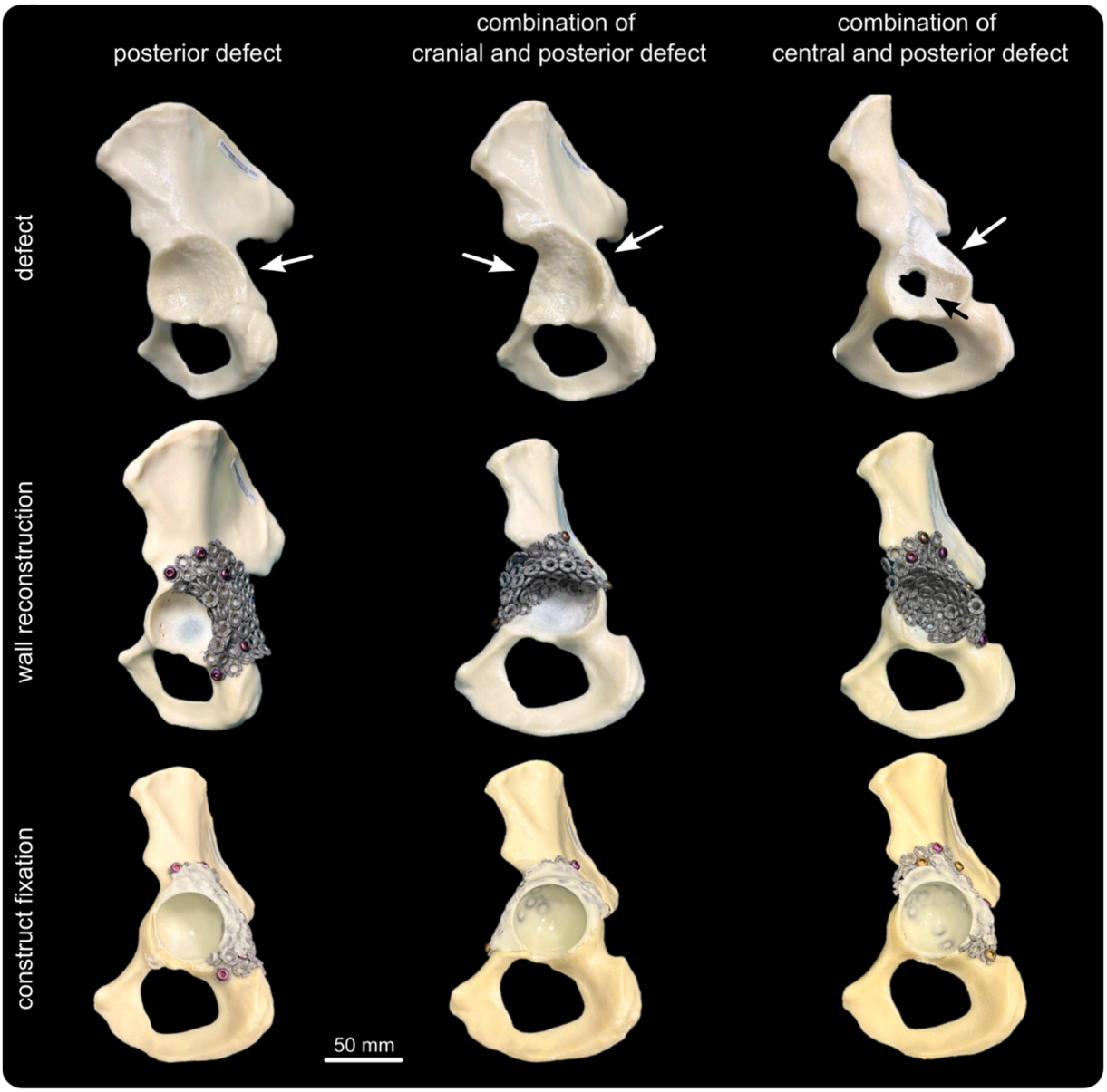

Fig. 2. Reconstruction of acetabular defects using the shape-morphing mesh implant. The flexible mesh implant reconstructed three types of acetabular defects (posterior, cranial, posterior combination, and central and posterior combination). The top row shows the original defects (indicated by arrows), the middle row shows the mesh-based wall reconstruction, and the bottom row illustrates the final construct fixation with an acetabular cup.

Refobacin® Bone Cement R, Zimmer Biomet, BIOMET France, France) was applied to the prepared acetabular surface. The bone cement was introduced, followed by pressurization to ensure optimal distribution (Supplementary video 4). To further enhance stability and support, bone impaction grafting can be added between the posterior mesh part and the anterior mesh part (Supplementary video 3). The size of the acetabular cup (46 mm in diameter), chosen by the surgeon to suit the reconstruction, was simulated using a punch of matching dimensions. Applying bone cement helped lock the mesh securely, providing additional mechanical support and ensuring the implant remained stable under load. After cement hardening the punch was retracted.

2.4. CT scanning and analysis

CT images were acquired using a TESCAN CorTOM CT scanner (TESCAN, Brno, Czech Republic), and the resulting images were analyzed and segmented using Dragonfly image processing software (version 2022.1.1249), applying Otsu method to optimize the thresholding for segmentation accuracy. Each specimen was scanned over a full 360° rotation, with an isotropic voxel size of 45 μm and an angular rotation step of 0.08°. The CT images were acquired under a voltage of 150 kV and a current of 300 μA, with each imaging cycle taking ~14 min to complete.

The shape-matching performance of the flexible mesh implants was assessed by comparing post-surgery CT scans of the reconstructed acetabulum for three different defect types (*i.e.,* posterior defect, a combination of posterior and cranial defects, and a combination of central and posterior defects) (Fig. 3a), with a healthy, intact acetabulum model featuring a 52 mm femoral head.

To evaluate the surface conformity of the mesh implants to the acetabulum, the degree of conformity was quantified by measuring the distance between the implant and the bone surface of a healthy, intact hemipelvis model. CloudCompare software (V.2.9.1) was used to align the implanted hemipelvis with the healthy model, and the distance between the two surfaces was calculated (Fig. 3b). In addition, a sphere-fitting method was applied by selecting 30 points within the acetabular cavity to determine the maximum size of a sphere that could be fitted into the reconstructed acetabulum (Fig. 3c). This sphere-fitting process provided additional insights into the volumetric accuracy and fit of the implant within the acetabular structure.

2.5. Biomechanical testing

Biomechanical testing was conducted using 18 synthetic hemipelvis samples to evaluate the load-bearing capacity and durability of the implants. The samples were divided equally into two groups: one group for quasi-static compression tests and the other for cyclic loading tests. Within each group, three samples were allocated to each of the three defect types (posterior wall, cranial-posterior combination, and central-posterior defects). A custom setup (Synbone AG, Switzerland) was used for all the tests to ensure consistent positioning and alignment of the synthetic hemipelvis models. The hemipelvis models were secured at both the ilium and pubic regions, with the acetabular cavity oriented upward to facilitate uniaxial compression testing (Fig. 4a). The vertical compressive load was applied directly to the acetabulum, simulating the quasi-static tests that represented increasing loads during quiet standing, while the cyclic loading tests simulated partial body weight support during standing.

A mechanical testing machine (LLOYD Instrument LR5K, Hampshire, United Kingdom) equipped with a 5 kN load cell was employed for the quasi-static uniaxial compression tests. Each sample was compressed at a 1 mm/min rate, ensuring precise alignment and stability through the custom setup. Displacement, force, and time were continuously recorded at a sampling rate of 100 Hz. The tests were conducted until either the implant or hemipelvis failed or a vertical displacement of 30 mm was reached. A preload of 10 N was applied at the start of each test. For each sample, the maximum load, displacement, and failure modes were collected to assess the initial mechanical stability of the implants.

Cyclic compression-compression testing was performed using an electrodynamic mechanical testing machine (ElectroPulse™ E10000, Instron, MA, USA) with a 10 kN load cell. Each sample was subjected to cyclic loading at a frequency of 2 Hz, following two loading scenarios: an initial maximum load of 350 N, followed by a 25 % increase to 437.5 N [46–48]. A constant load ratio of 0.1 (*i.e.,* the ratio of minimum to maximum loads in each cycle) was applied, and each step consisted of 500,000 cycles (Fig. 4e). Displacement, signs of fatigue failure, and implant migration were continuously monitored to evaluate the long-term durability of the mesh implants.

2.6. Statistical analysis

Statistical analysis was performed using OriginPro (2023, OriginLab Corporation, Northampton, MA, USA) to analyze the maximum difference between the reconstructed acetabulum and the healthy model, mechanical strength, and sphere-fitting data. Mean values and standard deviations were calculated to summarize the data. Due to the small sample size ($n = 3$ per group), non-parametric tests (*i.e.,* Kruskal-Wallis test) were employed where appropriate, with a significance level of 0.05 used for comparisons. The results should be interpreted with caution, and future studies with larger sample sizes are recommended to validate these findings.

3. Results

3.1. Shape-matching performance

For the posterior defect, the shape-morphing implant demonstrated close conformity, with a maximum distance of 9.5 mm (±0.6) from the healthy acetabulum. In the combination defect, where both cranial and posterior walls were compromised, the maximum distance was 10.1 mm (±0.6), reflecting a comparable level of fit despite the increased complexity. The mesh exhibited the highest level of conformity for the central and posterior defect, with a maximum distance of 8.3 mm (±1.3), indicating a more precise adaptation to the defect geometry (Fig. 3b). In all cases, the maximum distances were observed at the edges of the acetabulum.

In addition to surface gap measurements, a sphere-fitting analysis was conducted to determine the maximum sphere size that could be accommodated within the reconstructed acetabulum for each defect type. The sphere fitted to the healthy acetabulum was 53.8 mm. For the posterior defect, the maximum sphere diameter was 50.3 mm (±2.8), closely matching the capacity of the healthy acetabulum and closely approximating the capacity of the healthy acetabulum. The sphere size remained consistent at 50.4 mm (±1.5) in the cranial and posterior combination defect. For the central and posterior defect, the sphere size was slightly reduced to 49.5 mm (±0.7), indicating that the mesh restored a significant portion of the acetabular volume.

3.2. Biomechanical performance

Quasi-static uniaxial compression tests demonstrated that the pelvic constructs with flexible mesh implants could withstand substantial loads before failure. The mean maximum load capacities were 1890.9 N (±112.3) for the posterior defect, 1501.6 N (±142.5) for the cranial-posterior combination defect, and 1923.7 N (±199.3) for the central-posterior defect. The corresponding stiffness values for the mesh-pelvis constructs were 239 N/mm (±0.8) for the posterior defect, 237.8 N/mm (±0.9) for the cranial-posterior combination defect, and 198 N/mm (±0.2) for the central-posterior defect. Displacement at both the maximum load and the point of failure was consistent across all the specimens, indicating a uniform response to applied loading. Failure modes observed in all the tested specimens primarily involved fractures

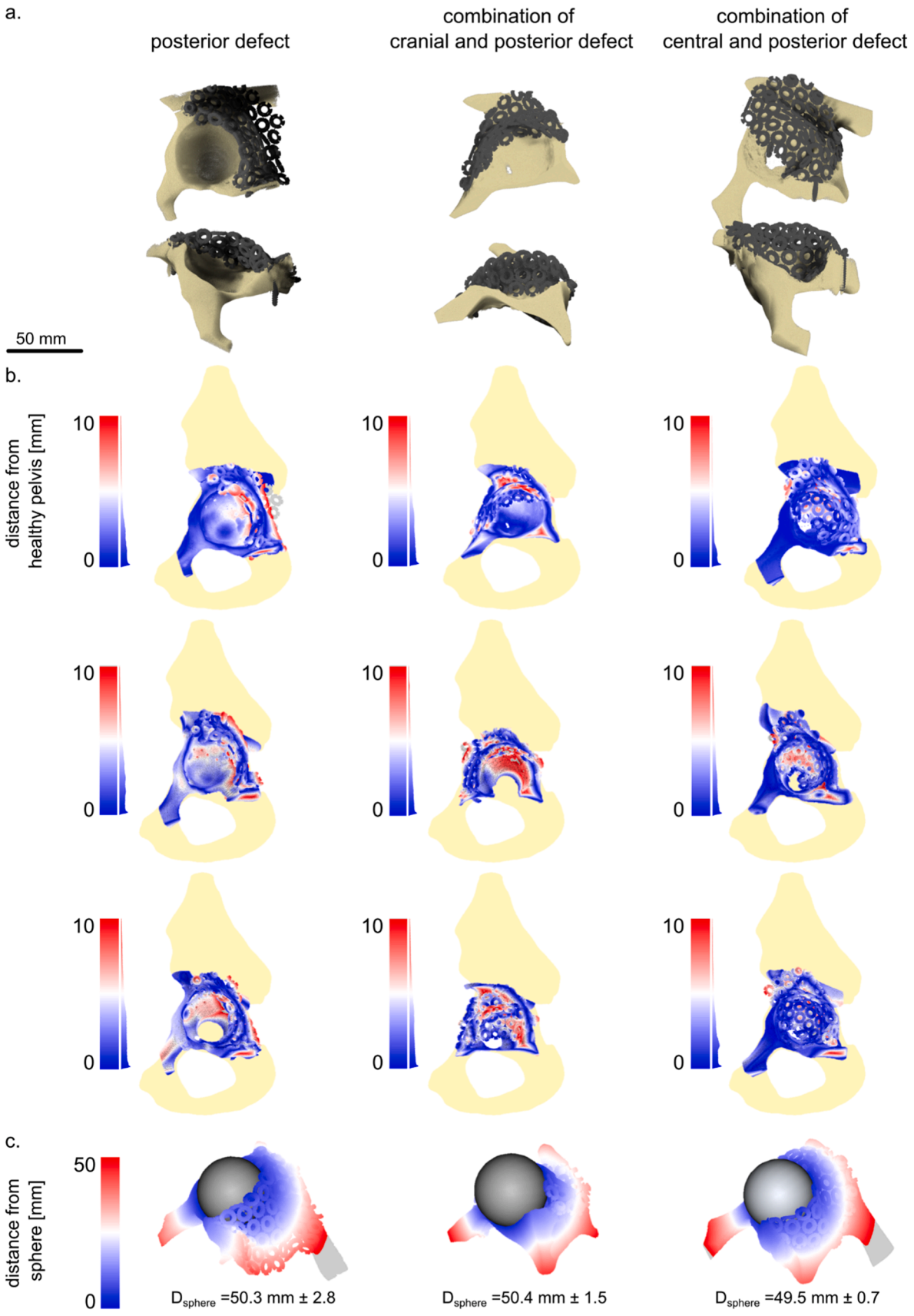

Fig. 3. Shape-matching performance and sphere-fitting analysis of the shape-morphing mesh implants. (a) 3D reconstructions of the flexible mesh implants from μCT images, fitted to the posterior, cranial-posterior, and central-posterior acetabular defects post-surgery. (b) The distance between each defect type's reconstructed acetabulum and the healthy pelvis. (c) A sphere-fitting analysis showing the maximum sphere diameter (D_{sphere}) that the reconstructed acetabulum for each defect type can accommodate.

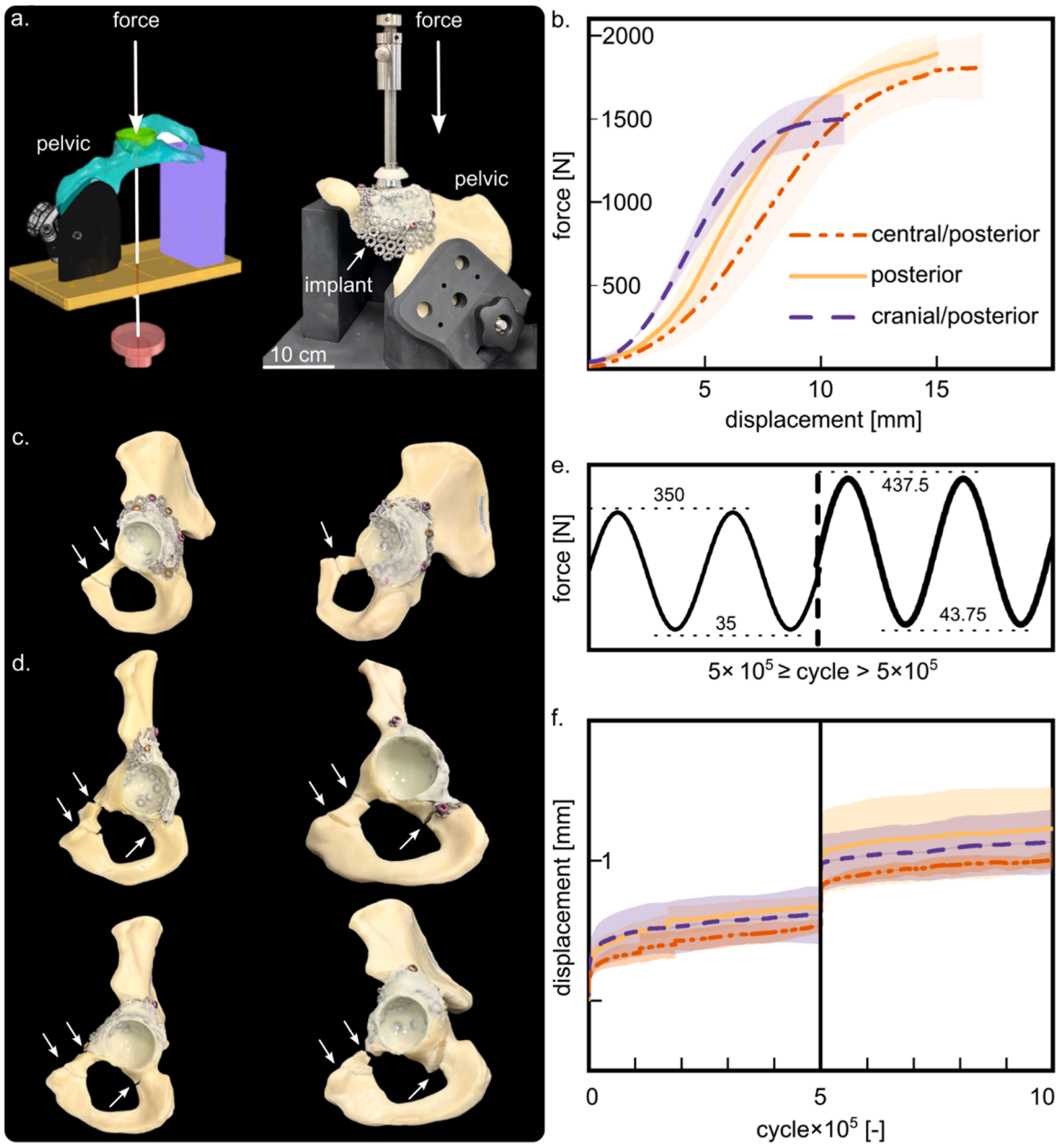

Fig. 4. Biomechanical testing of shape-morphing implants for acetabular defects. (a) A schematic drawing and experimental setup for uniaxial compression testing of the synthetic hemipelvis models with flexible mesh implants. The compressive force was applied vertically to the acetabulum. (b) Force-displacement curves for the three acetabular defect types (central/posterior, posterior, and cranial/posterior) during quasi-static compression testing. (c) First observed failure points under compression testing, with fractures occurring in the pubic region while the mesh and bone cement remained intact. (d) After initial failure, compression testing was extended to observe further failure points. All the specimens exhibited subsequent fractures in the synthetic bone without damage to the mesh or cement interfaces. (e) The protocol for the cyclic testing of the mesh-pelvis constructs was conducted in two phases (each up to 500,000 cycles) with forces of 350 N and 437.5 N at a frequency of 2 Hz. (f) Results from the cyclic testing, represented by extension-cycle curves, highlighting the durability and long-term performance of the flexible mesh implants under repetitive loading conditions.

of the synthetic bone, specifically starting at the superior ramus of the pubis, followed by fractures at the pubic tubercle (Fig. 4c).

The tests were extended to identify additional failure points and potentially weak areas within the pelvis-mesh construct. For both the posterior defect and the central and posterior defect, increased displacement revealed subsequent weak points at the screw locations, particularly those in the superior ischial ramus (Fig. 4d-top). Interestingly, for the combination defect, where no screws were positioned in the ischium, fractures still occurred at the superior ischial ramus after the initial breakage at the pubis (Fig. 4d-bottom). This suggests that the superior ischial ramus is inherently the next failure point, regardless of whether screws are used in this region. No cracks or visible changes were observed in the flexible mesh or the bone cement throughout the testing.

During cyclic testing, the mesh implants maintained their structural integrity under two loading phases, with maximum loads of 350 N and 437.5 N for up to 500,000 cycles per phase (*i.e.*, a total of >1000,000 loading cycles). Displacement changes were minimal at each step (*i.e.*, 0.38 mm, 0.46 mm, and 0.35 mm displacement after the first phase, and 0.27 mm, 0.28 mm, and 0.22 mm displacement after the second phase, for the central-posterior defect, posterior defect, and cranial-posterior combination defect, respectively). No sign of implant migration, screw loosening, or crack on the bone cement was observed throughout the test

cycles (Fig. 4f).

4. Discussion

This study evaluated the effectiveness of a 3D printed shape-morphing implant designed with kinematic structures to address complex acetabular defects. The results demonstrated that the flexible mesh provided a high degree of anatomical conformity, mechanical stability, and adaptability, which are critical factors in the success of acetabular reconstruction [49,50]. By focusing on three distinct defect types (*i.e.,* posterior wall, cranial-posterior combination, and central-posterior defects), the research provides comprehensive insights into the performance of the mesh in a range of clinically relevant scenarios.

The flexible nature of the mesh allowed it to conform closely to the irregular surfaces of the acetabulum (Fig. 1c). Minimal differences were observed between the reconstructed and healthy acetabula, with maximum surface discrepancies of 9.5 mm (±0.6) for the posterior defect, 10.1 mm (±0.6) for the cranial-posterior combination defect, and 8.3 mm (±1.3) for the central-posterior defect. The most significant discrepancies occurred at the acetabular edges, where the reconstructed wall was slightly higher than the natural acetabulum (Fig. 3b). This additional height enhances the acetabular cup's support, improving overall stability. The other more significant discrepancies observed at the acetabulum corresponded to the defect regions, which were absent compared to the healthy acetabulum (Fig. 3b).

The high degree of anatomical conformity is essential for ensuring stability and minimizing implant migration [51,52]. The mesh design provided a tailored fit for various defect shapes and sizes without requiring custom manufacturing for each patient. In contrast, while providing structural support, standard implants often require extensive bone reaming to fit properly (*e.g.,* 15,997 mm^3 for the trabecular metal acetabular revision system (TMARS) and 2292 mm^3 for a custom tri-flanged acetabular component (CTAC)) [25,53]. In our approach, the flexible mesh implant significantly reduces the need for reaming, as it adapts to complex anatomical geometries without extensive bone removal. While some reaming was performed to improve cement integration and provide adequate support for the acetabular cup, the process is far less invasive compared to traditional methods. Similar to patient-specific implants, which reduce reaming through improved anatomical conformity [54], the flexible mesh implant preserves bone stock, a critical advantage in cases of severe bone loss. These results highlight the ability of the meshes to adapt to different defect geometries while maintaining a close fit, which is essential for proper load distribution and implant stability.

Additionally, the sphere-fitting analysis further confirmed the capacity of the mesh design to restore acetabular volume with near-identical sphere sizes compared to the healthy model (Fig. 3c). However, no statistically significant difference was observed in sphere sizes between the defect groups. Similarly, there was no statistically significant difference in surface conformity between the different models. This level of shape-matching performance across varying defect types demonstrates the versatility of the mesh in adapting to different anatomical challenges while providing a secure and anatomically accurate fit. However, due to the volumetric effect of the mesh, selecting a slightly smaller cup would be better suited to maintain an optimal cement layer thickness. These outcomes suggest that the flexible mesh can closely replicate the anatomical structure, which is vital for the long-term success of THA in patients with significant bone loss [55,56].

The fixation of the flexible mesh implant relies on a combination of screws and bone cement. In this study, the number and location of the screws were chosen by the surgeon based on the specific anatomical requirements of each defect. Importantly, screws can be placed anywhere on the mesh according to the surgeon's preference, providing flexibility in the fixation strategy. While we used bone cement was to stabilize the mesh in the acetabular fossa, a screw can also be placed to support the mesh in the fossa if additional fixation is required. This flexibility allows the surgeon to tailor the fixation strategy to the patient's specific needs. The parts of the mesh that are not secured by screws are designed to conform to the bone surface and are stabilized by bone cement. While this method provides sufficient stability in the current study, the long-term reliability of fixation, particularly in areas not secured by screws, requires further investigation. Future studies should evaluate the potential effects of unsecured structures on implant performance under physiological loading conditions. Additionally, the use of bone cement in the acetabular fossa provides additional stability, but its reliability compared to existing fixation methods should be further explored. It is also worth noting that unsecured parts of the mesh could be removed if deemed unnecessary by the surgeon. However, the effects of removing these parts on the overall stability and performance of the implant requires further study.

The flexible mesh is designed to be compatible with a revision acetabular cup and UHMWPE bearing, offering a versatile solution for complex acetabular defects. The screws can be passed through the mesh to secure the cup to the host bone. The mesh does not restrict the trajectory of the screws, as the flexible design allows for screw placement at various angles, depending on the surgeon's preference and the patient's anatomy. This adaptability ensures that the mesh can be tailored to a wide range of clinical scenarios. While the current study did not explicitly evaluate the compatibility of the mesh with other components, further investigation is needed to demonstrate the feasibility of screw placement through the mesh during surgery and to evaluate the performance of the mesh in combination with a revision cup and screws. This includes studying different defect types, screw trajectories, and loading conditions to ensure optimal fixation and long-term stability.

The biomechanical tests indicated that the mesh implants could withstand high compressive loads, similar to the forces experienced in the hip joint (Fig. 4b). Importantly, none of the samples failed at the mesh, cement, or mesh-cement interfaces. Instead, all failures occurred in the synthetic bone at the superior pubic ramus and pubic tubercle (Fig. 4c). After the initial failure, the quasi-static tests were extended until a deflection of 30 mm, and subsequent failures consistently occurred in the pubic region of the synthetic bone, confirming that the mesh, cement, and mesh-cement interfaces remained intact throughout (Fig. 4d). In the cranial-posterior defect, the presence of screws in the pubic region resulted in earlier fractures at this location, which was attributed to the use of screws in that area. However, this failure occurred at the same location as the other defects, indicating that the mesh provided consistent performance across different anatomical scenarios. Statistical analysis using the Kruskal-Wallis test revealed no statistically significant differences in mechanical strength between the defect types ($p > 0.05$).

Cyclic loading tests further validated the durability of the mesh implants, revealing minimal performance degradation over time. The tests were conducted at maximum loads of 350 N and 437.5 N, representing approximately half the body weight of an 80 kg patient. While these loads are lower than the peak forces experienced during activities such as walking or running (which can exceed 2-3 times body weight [57]), they were chosen to avoid premature failure of the synthetic bone models, which have lower mechanical strength compared to human bone. The primary goal of the cyclic testing was to evaluate the long-term durability of the implant under repetitive loading rather than to replicate full physiological conditions. The results demonstrated that the flexible mesh implants maintained their structural integrity over 1000,000 cycles (equivalent to the approximate number of cycles experienced by active patients in one year [58]), with no signs of fatigue failure, screw loosening, or cement cracking. However, it is important to note that the magnitude of the loads used in the tests was lower than those experienced during activities such as walking or running because the synthetic bone models used in this study do not fully replicate the mechanical properties of the human bone, particularly the integration of bone cement with cancellous bone.

While a control group using intact bone or conventional meshes (*e.g.*,

Noviomagus) could provide additional insights, such comparisons were not feasible in this study. For intact bone, a larger punch size would be required to fit the acetabulum, and the absence of bone cement would result in a different connection scenario, making the design incomparable. Additionally, the defects studied here (posterior wall, cranial-posterior combination, and central-posterior defects) are not typically treated with conventional meshes, as they often require patient-specific implants to cover the defect area adequately. The objective of this study was not to claim superiority over existing designs but to demonstrate that the proposed flexible mesh can cover large defects without the need for patient-specific customization, offering a cost- and time-efficient solution for complex acetabular defects.

In cases like Paprosky type IIIB defects, acetabular fixation is particularly challenging due to the lack of superior dome support and proximal migration of the acetabular component [50]. Studies have demonstrated that using a hemispherical porous-coated component alone often leads to failure in these scenarios, primarily due to micro-motion and superolateral migration, especially when structural grafts or augmentations are not employed [59,60]. The standard BIG with mesh technique is usually unsuitable for type IIIB defects and is likely to have higher failure rates in type IIIA reconstructions [31]. The flexible mesh used in this study addresses these limitations by improving both conformity and stability. However, successful reconstruction still requires bone grafts, particularly in complex defects where restoring bone stock is crucial for long-term success [4,56,61].

A significant advantage of the flexible mesh design is its ability to accommodate bone grafts during surgery (Supplementary Video 3). The mesh allows easy manipulation, enabling precise placement within the defect while incorporating bone graft material beneath and between the mesh layers. This flexibility promotes better graft integration with surrounding tissue, enhancing long-term mechanical support and stability. During surgery, the mesh facilitates free movement, allowing for accurate positioning and even distribution of the bone graft, further improving osseointegration.

The surgical procedure for implanting the shape-morphing mesh is expected to be comparable to or shorter than that of custom-made implants, as the flexible mesh reduces the need for extensive bone reaming and intraoperative adjustments. If the surgeon is familiar with the design, the procedure could be implemented efficiently and would be comparable to custom implants in terms of surgical time. Additionally, the bone structure can be extracted from patient data and 3D-printed using standard 3D printers, allowing (less experienced) surgeons to practice the procedure and plan the fixation of the implant before the actual surgery. This preoperative planning could further reduce surgical time and improve outcomes. However, further studies are needed to quantify the surgical times and assess the potential impact on perioperative infection risk.

The ability of our flexible mesh implants to conform to different acetabular geometries and provide stable fixation has significant clinical implications. While severe defects, such as those we addressed in this study, typically require patient-specific meshes due to their complexity, our flexible mesh effectively covered these defects without requiring individualized manufacturing. This adaptability allows surgeons to use these implants in a broader range of patients, reducing the necessity for custom solutions and decreasing surgical wait times and overall treatment costs [5,62]. Future studies could enhance implant performance by exploring diverse network geometries and incorporating variable strut lengths within the structure. These adjustments could improve anatomical conformity and optimize load distribution, allowing the implants to better align with individual anatomical curvatures.

Despite the promising results, our study has limitations. The evaluation was conducted on synthetic hemipelvis models, which, while useful for controlled testing, do not fully replicate the complexities of the human bone. These limitations may have influenced the results of the quasi-static and cyclic loading tests, particularly the super-physiological deflection observed during failure. Notably, synthetic bone lacks cancellous bone, which is critical in integrating bone cement. In real-world scenarios, proper integration with cancellous bone can significantly enhance long-term implant stability, a factor not represented in our study. Further research using more advanced models or cadaveric specimens and clinical trials is necessary to further validate these findings under higher, more physiologically relevant loads and assess the added stability provided by bone-cement integration.

This study also focused on a single loading scenario during mechanical testing. Future research should consider various loading conditions that simulate the dynamic forces experienced in the hip joint during daily activities such as walking and running to evaluate the flexible mesh implants' performance fully. Moreover, the long-term *in vivo* performance of the shape-morphing implants was not assessed. Future research should also focus on the biocompatibility and durability of the implants over extended periods in living subjects.

5. Conclusions

This study successfully designed and evaluated 3D printed shape-morphing implants with kinematic structures for managing acetabular defects. The flexible mesh implants demonstrated high surface conformity and robust mechanical stability, adapting closely to the acetabulum and withstanding significant compressive loads. This flexible mesh offers improved adaptability and reduced need for extensive bone preparation, addressing some limitations of standard and custom implants. The 3D printed flexible mesh implants offer an efficient solution for acetabular defects of various sizes up to Paprosky IIIB, potentially significantly improving flexibility for the surgeon and offering new possibilities in orthopedic reconstruction surgery. Further research and clinical validation are essential to realize this innovative design's benefits fully.

CRediT authorship contribution statement

Vahid Moosabeiki: Writing – original draft, Visualization, Validation, Software, Methodology, Investigation, Formal analysis, Data curation, Conceptualization. **Marius A. Leeflang:** Writing – review & editing, Methodology, Investigation, Formal analysis, Conceptualization. **Jasper G. Gerbers:** Writing – review & editing, Methodology, Investigation, Formal analysis. **Pier H. de Jong:** Investigation. **Demien Broekhuis:** Writing – review & editing, Investigation. **Yash Agarwal:** Investigation. **Jagathes N. Ganesen:** Investigation. **Bart L. Kaptein:** Writing – review & editing, Investigation. **Rob G.H.H. Nelissen:** Writing – review & editing, Investigation. **Mohammad J. Mirzaali:** Writing – review & editing, Supervision, Methodology, Investigation, Formal analysis, Conceptualization. **Amir A. Zadpoor:** Writing – review & editing, Supervision, Resources, Methodology, Investigation, Funding acquisition, Formal analysis, Conceptualization.

Declaration of competing interest

A patent application has been filed that is partially based on the results of the current study.

The authors declare that they have no known competing financial interests or personal relationships that could have appeared to influence the work reported in this paper.

Amir A. Zadpoor is an Editorial Board Member for this journal and was not involved in the editorial review or the decision to publish this article.

Acknowledgments

The authors thank Eric Garling from Stryker Corporation for his insightful feedback during the preparation of this work. They also extend their appreciation to Arjan Thijssen from the Department of Materials, Mechanics, Management & Design at Delft University of

Technology for his support with the μCT scanning. This publication is part of the project “Metallic Clay: Shape-Matching Orthopaedic Implants” with file number 16582 of the research programme Vidi TTW which is financed by the Dutch Research Council (NWO).

Supplementary materials

Supplementary material associated with this article can be found, in the online version, at doi:10.1016/j.actbio.2025.07.018.

References

[1] M. Baauw, M.L. van Hooff, M. Spruit, Current construct options for revision of large acetabular defects: a systematic review, JBJS. Rev. 4 (11) (2016) e2.

[2] F. Mancino, G. Cacciola, V. Di Matteo, D. De Marco, A. Greenberg, C. Perisano, M. Ma, P.K. Sculco, G. Maccauro, I. De Martino, Reconstruction options and outcomes for acetabular bone loss in revision hip arthroplasty, (2035-8237 (Print)).

[3] A.G. Chen, Total Hip Arthroplasty in Young Patients, The University of Western Ontario (Canada, 2022.

[4] W.Y. Shon, S.S. Santhanam, J.W. Choi, Acetabular Reconstruction in Total Hip Arthroplasty, (2287-3260 (Print)).

[5] D. Broekhuis, W.M.H. Meurs, B.L. Kaptein, S. Karunaratne, R.L. Carey Smith, S. Sommerville, R. Boyle, R.G.H.H. Nelissen, High accuracy of positioning custom triflange acetabular components in tumour and total hip arthroplasty revision surgery, Bone Jt. Open. 5 (4) (2024) 260–268.

[6] J.A. Shaw, A. Bailey Jh Fau - Bruno, R.B. Bruno A Fau - Greer, 3rd, R.B. Greer, 3rd, Threaded acetabular components for primary and revision total hip arthroplasty, (0883-5403 (Print)).

[7] P.K. Sculco, T. Wright, M.A. Malahias, A. Gu, M. Bostrom, F. Haddad, S. Jerabek, M. Bolognesi, T. Fehring, A. Gonzalez DellaValle, W. Jiranek, W. Walter, W. Paprosky, D. Garbuz, T. Sculco, The Diagnosis and Treatment of Acetabular Bone Loss in Revision Hip Arthroplasty: An International Consensus Symposium, (1556-3316 (Print)).

[8] D.G. Allan, A. Bell Rs Fau - Davis, F. Davis A Fau - Langer, F. Langer, Complex acetabular reconstruction for metastatic tumor, (0883-5403 (Print)).

[9] B.N. Trumm, S.S. Callaghan Jj Fau - Liu, D.D. Liu Ss Fau - Goetz, R.C. Goetz Dd Fau - Johnston, R.C. Johnston, Revision with cementless acetabular components: a concise follow-up, at a minimum of twenty years, of previous reports, (1535-1386 (Electronic)).

[10] C.L. Sheth Np Fau - Nelson, B.D. Nelson Cl Fau - Springer, T.K. Springer Bd Fau - Fehring, W.G. Fehring Tk Fau - Paprosky, W.G. Paprosky, Acetabular bone loss in revision total hip arthroplasty: evaluation and management, (1067-151X (Print)).

[11] B.T. Barlow, G.H. McLawhorn As Fau - Westrich, G.H. Westrich, The Cost-Effectiveness of Dual Mobility Implants for Primary Total Hip Arthroplasty: A Computer-Based Cost-Utility Model, (1535-1386 (Electronic)).

[12] S.G. Brouwer de Koning, N. de Winter, V. Moosabeiki, M.J. Mirzaali, A. Berenschot, M.M.E.H. Witbreuk, V. Lagerburg, Design considerations for patient-specific bone fixation plates: a literature review, Med. Biol. Eng. Comput. 61 (12) (2023) 3233–3252.

[13] M.D. Ries, Reconstruction and Management Options For Acetabular Bone Loss, Fundamentals of Revision Hip Arthroplasty, CRC Press, 2024, pp. 91–101.

[14] P.S. Issack, M. Nousiainen, B. Beksac, D.L. Helfet, T.P. Sculco, R.L. Buly, Acetabular component revision in total hip arthroplasty. Part II: management of major bone loss and pelvic discontinuity, Am. J. Orthop. (Belle Mead. NJ) 38 (11) (2009) 550–556.

[15] D. Broekhuis, R. Tordoir, Z. Vallinga, J. Schoones, B. Pijls, R. Nelissen, Custom triflange acetabular components for large acetabular defect reconstruction in revision total hip arthroplasty: a systematic review and meta-analysis on 1218 patients, EFORT. Open. Rev. 8 (7) (2023) 522–531.

[16] J.-A. Lee, Y.-G. Koh, K.-T. Kang, Biomechanical and clinical effect of patient-specific or customized knee implants: a review, J. Clinical Med. 9 (5) (2020) 1559.

[17] L. Dall'Ava, H. Hothi, A. Di Laura, J. Henckel, A. Hart, 3D printed acetabular cups for total hip arthroplasty: a review article, Metals 9 (7) (2019) 729.

[18] S.-H. Woo, M.-J. Sung, K.-S. Park, T.-R. Yoon, Three-dimensional-printing technology in hip and pelvic surgery: current landscape, Hip. Pelvis. 32 (1) (2020) 1–10.

[19] O. Okolie, I. Stachurek, B. Kandasubramanian, J. Njuguna, 3D printing for hip implant applications: a review, Polymers 12 (11) (2020) 2682.

[20] V. Goriainov, L.J. King, R.O. Oreffo, D.G. Dunlop, Custom 3D-printed triflange implants for treatment of severe acetabular defects, with and without pelvic discontinuity: early results of our first 19 consecutive cases, JBJS Open Access 6 (4) (2021) e21.

[21] A. Taninaka, T. Kabata, Y. Kajino, D. Inoue, T. Ohmori, Y. Yamamuro, T. Kataoka, Y. Saiki, Y. Yanagi, M. Ima, Accurate implant placement in THA using three-dimensional printed custom-made acetabular component for massive defects, Proceedings of The 22nd Annual Meeting of the Interna, 2024, pp. 110–114.

[22] S. Fang, Y. Wang, P. Xu, J. Zhu, J. Liu, H. Li, X. Sun, Three-dimensional-printed titanium implants for severe acetabular bone defects in revision hip arthroplasty: short-and mid-term results, Int. Orthop. 46 (6) (2022) 1289–1297.

[23] Z. Li, Y. Luo, M. Lu, Y. Wang, T. Gong, X. Hu, X. He, Y. Zhou, L. Min, C. Tu, 3D-printed personalized porous acetabular component to reconstruct extensive acetabular bone defects in primary hip arthroplasty, Orthop. Surg. (2024).

[24] C. Xiao, S. Zhang, Z. Gao, C. Tu, Custom-made 3D-printed porous metal acetabular composite component in revision hip arthroplasty with Paprosky type III acetabular defects: a case report, Technol. Health Care 31 (1) (2023) 283–291.

[25] S.A. Callary, D. Broekhuis, J. Barends, B. Ramasamy, R.G.H.H. Nelissen, L. B. Solomon, B.L. Kaptein, Virtual biomechanical assessment of porous tantalum and custom triflange components in the treatment of patients with acetabular defects and pelvic discontinuity, Bone Joint J. (2024) 74–81.

[26] S.J. Lee, J.J. Shea, Acetabular Apparatuses For Hip Revision Surgery, Google Patents, 2023.

[27] A.A.-O. Di Laura, J. Henckel, A. Hart, Custom 3D-printed implants for acetabular reconstruction: intermediate-term functional and radiographic results. LID - 10.2106/JBJS.OA.22.00120 [doi] LID - e22.00120, (2472-7245 (Electronic)).

[28] A.A. Zadpoor, Design for additive Bio-manufacturing: from patient-specific medical devices to rationally designed meta-biomaterials, Int. J. Mol. Sci. (2017).

[29] A. van Kootwijk, V. Moosabeiki, M.C. Saldivar, H. Pahlavani, M.A. Leeflang, S. Kazemivand Niar, P. Pellikaan, B.P. Jonker, S.M. Ahmadi, E.B. Wolvius, N. Tümer, M.J. Mirzaali, J. Zhou, A.A. Zadpoor, Semi-automated digital workflow to design and evaluate patient-specific mandibular reconstruction implants, J. Mech. Behav. Biomed. Mater. 132 (2022) 105291.

[30] V. Moosabeiki, N. de Winter, M. Cruz Saldivar, M.A. Leeflang, M.M.E.H. Witbreuk, V. Lagerburg, M.J. Mirzaali, A.A. Zadpoor, 3D printed patient-specific fixation plates for the treatment of slipped capital femoral epiphysis: topology optimization *vs.* conventional design, J. Mech. Behav. Biomed. Mater. 148 (2023) 106173.

[31] M.-A. Malahias, F. Mancino, A. Gu, M. Adriani, I. De Martino, F. Boettner, P. K. Sculco, Acetabular impaction grafting with mesh for acetabular bone defects: a systematic review, HIP Int. 32 (2) (2022) 185–196.

[32] M.J. Mirzaali, V. Moosabeiki, S.M. Rajaai, J. Zhou, A.A. Zadpoor, Additive manufacturing of biomaterials—Design principles and their implementation, Materials (2022).

[33] M.A. Leeflang, F.S.L. Bobbert, A.A. Zadpoor, Additive manufacturing of non-assembly deployable mechanisms for the treatment of large bony defects, Addit. Manuf. 46 (2021) 102194.

[34] T. van Manen, S. Janbaz, K.M.B. Jansen, A.A. Zadpoor, 4D printing of reconfigurable metamaterials and devices, Commun. Mater. 2 (1) (2021) 56.

[35] V. Moosabeiki, E. Yarali, A. Ghalayaniesfahani, S.J.P. Callens, T. van Manen, A. Accardo, S. Ghodrat, J. Bico, M. Habibi, M.J. Mirzaali, A.A. Zadpoor, Curvature tuning through defect-based 4D printing, Commun. Mater. 5 (1) (2024) 10.

[36] F.S.L. Bobbert, S. Janbaz, T. van Manen, Y. Li, A.A. Zadpoor, Russian doll deployable meta-implants: fusion of kirigami, origami, and multi-stability, Mater. Des. 191 (2020) 108624.

[37] P.H. de Jong, A.L. Schwab, M.J. Mirzaali, A.A. Zadpoor, A multibody kinematic system approach for the design of shape-morphing mechanism-based metamaterials, Commun. Mater. 4 (1) (2023) 83.

[38] S. Leeflang, S. Janbaz, A.A. Zadpoor, Metallic clay, Addit. Manuf. 28 (2019) 528–534.

[39] P.H. de Jong, Y. Salvatori, F. Libonati, M.J. Mirzaali, A.A. Zadpoor, Shape-locking in architected materials through 3D printed magnetically activated joints, Mater. Des. 235 (2023) 112427.

[40] F.S.L. Bobbert, S. Janbaz, A.A. Zadpoor, Towards deployable meta-implants, J. Mater. Chem. B 6 (21) (2018) 3449–3455.

[41] R.G. Nelissen, T.W. Bauer, L.R. Weidenhielm, D.P. LeGolvan, W.E. Mikhail, Revision hip arthroplasty with the use of cement and impaction grafting. Histological analysis of four cases, JBJS 77 (3) (1995).

[42] E. García-Rey, R. Madero, E. García-Cimbrelo, THA revisions using impaction allografting with mesh is durable for medial but not lateral acetabular defects, Clin. Orthopaed. Related Res. 473 (12) (2015).

[43] Y.-Y. Lian, F.-X. Pei, J.-Q. Cheng, W. Feng, H. Zhang, Reconstruction of acetabular defect with wire mesh and impacted bone graft in cemented acetabular revision], Zhonghua Yi Xue Za Zhi 87 (23) (2007) 1603–1606.

[44] W.H. Harris, W.N. Jones, The use of wire mesh in total hip replacement surgery, Clin. Orthopaed. Related Res. 106 (1975).

[45] M.C. Koper, N.M.C. Mathijssen, F. Witt, M.M. Morlock, S.B.W. Vehmeijer, Severe wear and pseudotumor formation due to taper mismatch in a total hip arthroplasty: a case report, JBJS Case Connect. 5 (2) (2015).

[46] L. Jin, X. Hao, Z. Zhang, Q. Zhang, S. Zhang, F. Zhou, S. Yang, W. Zheng, X. Xiong, W. Gong, Y. Wang, X. Chen, J. Huang, New minimally invasive method for treating posterior pelvic ring fractures: biomechanical validation and clinical application of sacroiliac joint locking plate, Orthopaedic Surgery (2024).

[47] T.A. Schildhauer, W.R. Ledoux, J.R. Chapman, M.B. Henley, A.F. Tencer, M.L. C. Routt Jr., Triangular osteosynthesis and iliosacral screw fixation for unstable sacral fractures: a cadaveric and biomechanical evaluation under cyclic loads, J. Orthop. Trauma. 17 (1) (2003).

[48] I. Graul, I. Marintschev, A. Pizanis, S.C. Herath, T. Pohlemann, T. Fritz, The effect of an infra-acetabular screw for anatomically shaped three-dimensional plate or standard plate designs in acetabulum fractures: a biomechanical analysis, Eur. J. Trauma Emerg. Surgery 48 (5) (2022) 3757–3764.

[49] G.W. Fryhofer, S. Ramesh, N.P. Sheth, Acetabular reconstruction in revision total hip arthroplasty, J. Clin. Orthop Trauma 11 (1) (2020) 22–28.

[50] A.Q. Ahmad, R. Schwarzkopf, Clinical evaluation and surgical options in acetabular reconstruction: a literature review, J. Orthop. 12 (2015) S238–S243.
[51] J. Thanner, The acetabular component in total hip arthroplasty: evaluation of different fixation principles, Acta Orthop. Scand. 70 (sup286) (1999) i–41.
[52] P.K. Sculco, T. Wright, M.-A. Malahias, A. Gu, M. Bostrom, F. Haddad, S. Jerabek, M. Bolognesi, T. Fehring, A. Gonzalez DellaValle, The diagnosis and treatment of acetabular bone loss in revision hip arthroplasty: an international consensus symposium, HSS J. 18 (1) (2022) 8–41.
[53] P.C. Krause, J.L. Braud, J.M. Whatley, Total hip arthroplasty after previous fracture surgery, Orthoped. Clinics 46 (2) (2015) 193–213.
[54] E. Garner, A. Meynen, L. Scheys, J. Wu, A.A. Zadpoor, Automated design of bone-preserving, insertable, and shape-matching patient-specific acetabular components, J. Orthopaed. Res. 42 (11) (2024) 2535–2544.
[55] F.S. Fröschen, T.M. Randau, G.T.R. Hischebeth, N. Gravius, S. Gravius, S.G. Walter, Mid-term results after revision total hip arthroplasty with custom-made acetabular implants in patients with Paprosky III acetabular bone loss, Arch. Orthop. Trauma Surg. 140 (2) (2020) 263–273.
[56] F. Mancino, G. Cacciola, V. Di Matteo, D. De Marco, A. Greenberg, C. Perisano, M. Malahias, P.K. Sculco, G. Maccauro, I. De Martino, Reconstruction options and outcomes for acetabular bone loss in revision hip arthroplasty, Orthop. Rev. 12 (Suppl 1) (2020).
[57] N. Hinz, J. Dehoust, M. Munch, K. Seide, T. Barth, A.P. Schulz, K.H. Frosch, M. J. Hartel, Biomechanical analysis of fixation methods in acetabular fractures: a systematic review of test setups, Eur. J. Trauma Emerg. Surg. 48 (5) (2022) 3541–3560.
[58] M. Morlock, E. Schneider, A. Bluhm, M. Vollmer, G. Bergmann, V. Müller, M. Honl, Duration and frequency of every day activities in total hip patients, J. Biomech. 34 (7) (2001) 873–881.
[59] S. Avci, N. Connors, W. Petty, 2-to 10-year follow-up study of acetabular revisions using allograft bone to repair bone defects, J. Arthroplasty. 13 (1) (1998) 61–69.
[60] M. Jasty, W.H. Harris, Total hip reconstruction using frozen femoral head allografts in patients with acetabular bone loss, Orthoped. Clinics North Am. 18 (2) (1987) 291–299.
[61] E. Garcia-Rey, L. Saldaña, E. Garcia-Cimbrelo, Impaction bone grafting in hip re-revision surgery: bone stock restoration and radiological migration of the acetabular component, Bone Joint J. 103 (3) (2021) 492–499.
[62] B.T. Barlow, A.S. McLawhorn, G.H. Westrich, The cost-effectiveness of dual mobility implants for primary total hip arthroplasty: a computer-based cost-utility model, JBJS 99 (9) (2017).